Supercond. Sci. Technol. **21** (2008) 115006 (6pp) doi:10.1088/0953-2048/21/11/115006

Deposition and characterization of few-nanometers-thick superconducting Mo–Re films

V A Seleznev[1], M A Tarkhov[1], B M Voronov[1], I I Milostnaya[1], V Yu Lyakhno[2], A S Garbuz[2], M Yu Mikhailov[2], O M Zhigalina[3] and G N Gol'tsman[1]

[1] Department of Physics, Moscow State Pedagogical University (MSPU), Moscow 119435, Russia
[2] B Verkin Institute for Low Temperature Physics and Engineering of the National Academy of Sciences of Ukraine (ILTPE), Kharkov 61103, Ukraine
[3] A V Shubnikov Institute of Crystallography Russian Academy of Sciences (ICRAS), Moscow 119333, Russia

E-mail: seleznev@rplab.ru

Received 4 May 2008, in final form 28 July 2008
Published 9 September 2008
Online at stacks.iop.org/SUST/21/115006

Abstract
We report on the fabrication and investigation of few-nanometers-thick superconducting molybdenum–rhenium (Mo–Re) films intended for use in nanowire single-photon superconducting detectors (SSPDs). Mo–Re films were deposited on sapphire substrates by DC magnetron sputtering of an Mo(60)–Re(40) alloy target in an atmosphere of argon. The films 2–10 nm thick had critical temperatures (T_c) from 5.6 to 9.7 K. HRTEM (high-resolution transmission electron microscopy) analysis showed that the films had a homogeneous structure. XPS (x-ray photoelectron spectroscopy) analysis showed the Mo to Re atom ratio to be 0.575/0.425, oxygen concentration to be 10%, and concentration of other elements to be 1%.

1. Introduction

In this paper, we study ultrathin molybdenum–rhenium (Mo–Re) films intended for nanowire superconducting single-photon detectors (SSPDs). The SSPDs are meander-shaped superconducting nanowires made from few-nanometers-thick superconducting films [1]. The SSPD operation is based on the formation of a photon-induced resistive hotspot in a current-carrying superconducting nanowire [2, 3]. SSPDs operate at a temperature well below the temperature T_c and are biased close to the critical current I_c of the nanowire at the operating temperature. Hence it is desirable to have superconducting films as thin as several nanometers with a fairly high T_c, a sharp superconducting transition and a high critical current density. So far, the material of choice for SSPDs has been niobium nitride (NbN) [1–11], and SSPDs made of ultrathin Nb films have been developed [7, 12]. NbN SSPDs made of high-quality epitaxially-grown NbN films (4 nm thick, T_c = 9–11 K, j_c = 6–7 × 10^6 A cm^{-2}) operate in a temperature range of 2–5 K (well below T_c); in the single-photon counting mode they offer a very low dark count rate and a very small jitter [4–6, 10]. The operating spectral range extends from the visible to the mid-IR. Although the quantum efficiency (QE) of the detectors decreases with increasing radiation wavelength, their sensitivity in the IR can be significantly improved by lowering the operating temperature to 2 K [6]. It is expected that SSPD performance in the mid- and far-IR ranges can be improved further by using narrow-gap superconductors with a low quasi-particle diffusivity. The use of a material with a low transition temperature should shift the detector's sensitivity towards longer wavelengths.

For the efficient operation of a detector we have to use ultrathin films. For example, the reduction of the NbN film thickness from 10 to 3.5 nm leads to about two orders of magnitude increase of quantum efficiency in the infrared. We attribute it to the larger size of the hotspot which appears after photon absorption [4, 13]. One may expect that for other materials the film thickness should be below 4 nm to provide the fabrication of an efficient detector.

To find such a material, we had to compare T_c of relatively thick NbN films with T_c of narrow-gap superconducting thick films, since there are few papers containing information about

Table 1. Superconducting transition temperature of Mo–Re films deposited at different levels of discharge power.

Discharge power (W)/current (A)	180/0.5	380/1.0	600/1.5		840/2.0	
Film thickness (nm)	4	4	4	10	4	10
T_c (K)	No superconductivity down to 4.2 K	No superconductivity down to 4.2 K	7.4	8.8	7.7	9.7
ΔT_c (K)	No superconductivity down to 4.2 K	No superconductivity down to 4.2 K	0.2	0.1	0.3	0.2

few-nm-thick films. The critical temperature of the 6 μm thick Mo–Re films reaches 15 K [14], and for a rather thick NbN film T_c reaches 17 K [15]. As we can see, the difference in T_c between these materials is not so great, but T_c of Mo–Re films decreases more sharply than for NbN films as the film thickness decreases. For ultrathin films this difference may reach 4–5 K. So, it can be expected that Mo–Re SSPDs will be more sensitive in the far-IR range than NbN SSPDs.

The fabrication of few-nanometers-thick superconducting films with the desired properties is a challenge, since superconductivity degrades with the decrease in film thickness. The challenge is to obtain ultrathin films with properties most close to those for a bulk material. In this respect, a promising superconducting material may be an Mo–Re alloy, since single-crystalline films of this alloy as thin as 20 nm have a T_c of about 12 K [16]. The critical temperature of Mo–Re films depends on the Mo-to-Re ratio (it reaches the maximum value at the Mo 60% and Re 40% ratio) [17, 18] and structure, while their structure depends on the substrate temperature during deposition [14, 17, 18]. The deposition of Mo(60)–Re(40) thin films by magnetron sputtering was developed more than a decade ago [19]. The films exhibited a sharp superconducting transition, critical temperatures reaching 13 K and the single-crystalline A15 structure even at low deposition temperatures.

In this paper the first successful attempt to deposit few-nanometers-thick Mo–Re films suitable for SSPDs is reported. Mo–Re films with a thickness of 2–10 nm were deposited and thoroughly examined by the HRTEM method, GIXR (grazing incidence x-ray reflectivity) and XPS. Some preliminary results were published in [20].

2. Fabrication of ultrathin Mo–Re films

The MSPU team uses a well-established technique for the fabrication of SSPDs based on few-nm-thick NbN films [1, 4]. In the past, the team had experience in the fabrication of Mo–Re films with a relatively high thickness (300 nm and up) for applications for superconducting detectors [21]. An attempt to fabricate few-nm-thick Mo–Re films was made for the first time.

Mo–Re films were deposited on sapphire substrates by the DC magnetron sputtering of the Mo(60)–Re(40) alloy target in an argon atmosphere. The target–substrate distance was 70 mm. We used R-plane 0.4 mm thick sapphire substrates with epi-polished front sides and optically polished back sides. The deposition chamber was pumped down to the background pressure of 6×10^{-6} Torr. During the deposition process, the argon pressure was 3×10^{-3} Torr, while the substrate was heated to a temperature in the range from 150 to 600 °C. A magnetron was operated in a current stabilization mode at a current in the range from 0.5 to 2.0 A at a voltage of about 380 V.

Table 2. Dependence of the critical temperature of deposited films on the substrate temperature during the deposition.

Substrate temperature during the deposition (°C)	170	380	600
T_c (K)	4.75	7.0	6.2

To determine a deposition rate, we deposited relatively thick films and measured their thickness d using a *Talystep* profilometer–profilograph. Knowing the deposition rate and choosing the appropriate deposition time, we deposited films with the desired thickness.

The research was performed to achieve ultrathin Mo–Re films with possibly the highest superconducting transition temperature and critical current density. The film's quality depends on many deposition parameters such as the deposition rate, substrate temperature, etc. To optimize deposition conditions, we performed a series of experiments in which both the substrate temperature and discharge power were varied. The dependence of superconducting transition temperature on the discharge power during the deposition was investigated for 4 and 10 nm thick Mo–Re films. Several films were deposited at the same pressure of argon at discharge currents of 0.5, 1.0, 1.5 and 2.0 A (with correspondingly increasing values of the discharge power and deposition rate). The results presented in table 1 show that the films deposited at the increased discharge power are of high quality. It should be noted, however, that at a high discharge power the repeatability of deposition results drops for films thinner than 4–5 nm.

We also investigated the dependence of the superconducting transition temperature of the films on the substrate temperature. Several 4 nm thick Mo–Re films were deposited at a discharge power of 600 W at various substrate temperatures. The results shown in table 2 demonstrate that the highest T_c was achieved for the films deposited at a substrate temperature of 380 °C. Under such deposition conditions, the film deposition rate was 1.75 nm s^{-1}.

As a result, we managed to optimize the technique for the depositing ultrathin Mo–Re films. This technique allowed us to deposit Mo–Re films with a sharp superconducting transition (see figure 1) and good superconducting properties (high T_c and j_c), as shown further in table 3. We suppose that the maximum accessible values T_c and j_c at the defined

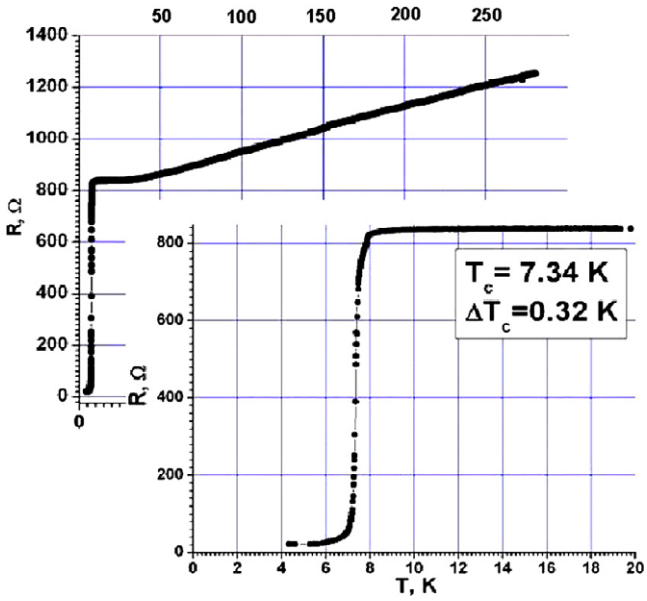

Figure 1. Superconducting transition of a 4 nm thick Mo–Re film.

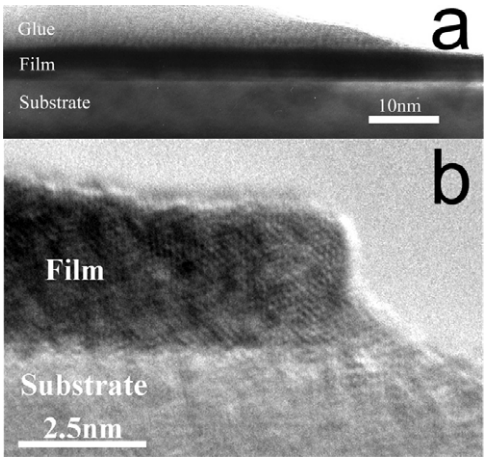

Figure 2. An HRTEM image of the cross section of an Mo–Re film specimen.

thickness were reached. Relatively small decrease in T_c and j_c (4.2 K) values compared to NbN made this material feasible for fabrication of SSPDs.

3. Structure and properties of fabricated Mo–Re films

The structure and properties of Mo–Re films were thoroughly investigated by different techniques including HRTEM, GIXR and XPS.

The HRTEM examination of 4 nm thick Mo–Re films was performed using Philips EM430 ST and Tecnai G^{2}30 S-TWIN transmission electron microscopes at an accelerating voltage of 200 kV and 300 kV, respectively. The cross-sectioned film specimens for HRTEM study were prepared by grinding, polishing, and ion beam milling in a Gatan-600 dual ion mill using 4 keV Ar^+ ions at angles of incidence from 14° to 10°.

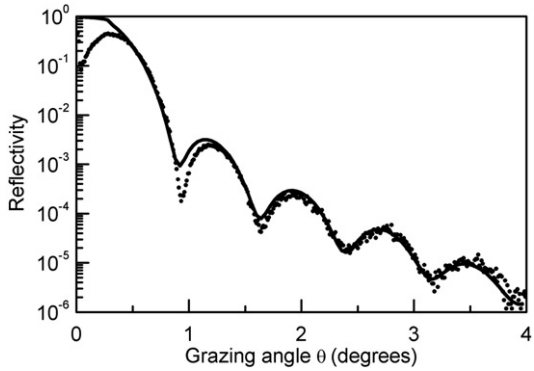

Figure 3. Measured (circles) and calculated (solid curve) grazing incidence x-ray reflectivity data for the 5.6 nm thick Mo–Re film.

Table 3. Properties of fabricated ultrathin Mo–Re films.

Film thickness (nm)	2	3	4	10
T_c (K)	4.2–5.2	4.4–6.5	5.2–7.7	9.7
ΔT_c (K)	0.1	0.1	0.2–0.3	0.2
$\rho_{300\ K}/\rho_{20\ K}$		1.2	1.38–1.49	
R_s ($\Omega/\square$)	120–190	77–117	52–69	26–28
ρ ($\mu\Omega$ cm)	24–38	23–35	21–28	26–28
$j_{c\ 4.2\ K}$ (μA cm^{-2})			1.1×10^6	
D (cm^2 s^{-1})			1.73	

The performed HRTEM analysis shows that:

- the films have a uniform structure without any breaks and exfoliations (figure 2(a));
- the observed film thickness is 4–5 nm (figure 2(a)). This means that the estimation of the film thickness from the deposition rate is correct (in figure 2(b) is shown the edge of the film, so we do not use it to estimate the film thickness);
- the film–substrate interface exhibits no angularity; the films exhibit homogeneous structure (figure 2(b)).

GIXR measurements were performed using a DRON-3M x-ray diffractometer utilizing Cu Kα1 radiation in the θ–2θ geometry. Figure 3 shows a typical measured reflectivity curve of the 5.6 nm thick Mo–Re film. An IMD software package [22] was used to fit experimental data on the reflectivity (figure 3). For 5.6 nm thick films the best-fit parameters were determined as follows: film density of 12.4 g cm^{-3}, roughness/diffuseness of the substrate of 0.325 nm and roughness/diffuseness of the film surface of 0.22 nm. The last value does not correspond to the crystal lattice parameter, since the orientation of the crystal layers was not defined.

The composition of Mo–Re films was studied by the XPS. 5.6 nm thick Mo–Re films were examined using a Riber SIA 100 system equipped with a modified cylindrical mirror analyzer with a retarding field. Photoelectron spectra were obtained with the Al Kα1 radiation ($h\nu$ = 1486.6 eV). The resolution of the spectrometer for the Au $4f_{7/2}$ peak (FWHM) was 1.6 eV. XPS sputter depth profiling was performed using 2.5–3.0 keV argon ion sputtering. The peak positions were referenced to the C 1s peak (284.6 eV). The background was

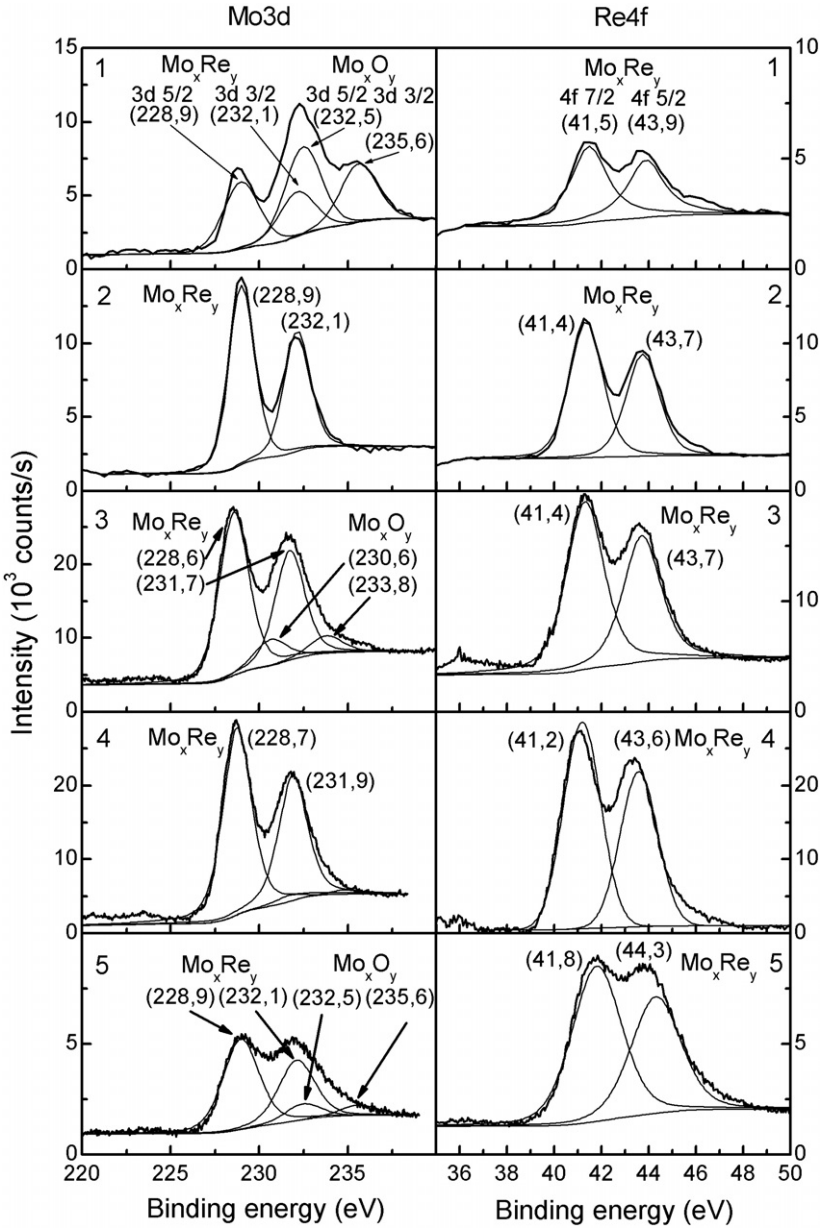

Figure 4. High energy resolution XPS spectra of deposited Mo–Re films: spectra for the surface of a thick film ($d \sim 100$ nm) after a long contact with ambient air (1); spectra taken after the sputter depth profiling of the thick film (2); spectra for the surface of the 5.6 nm thick film (3); spectra taken after the sputter depth profiling of the 5.6 nm thick film at half the thickness of the film (4) and near the film–substrate interface (5).

subtracted using the Shirley method. XPS peaks were fitted using the Gaussian–Lorentzian method.

Figure 4 shows the deconvoluted XPS spectra of Mo 3d and Re 4f bands. The experimental data for the Mo 3d band can be adequately fitted using two pairs of peaks: the first is associated with an Mo–Re compound (Mo $3d_{5/2}$ peak at binding energy 228.9 eV) and the other one with a molybdenum oxide (Mo $3d_{5/2}$ peak at binding energy 232.5 eV, graph 1 of figure 4). We observe a chemical shift of 1.2 eV for the Mo–Re compound compared to pure Mo. Mo 3d peak positions for a 5.6 nm thick film slightly changed with sputter depth profiling, suggesting that the stoichiometry of the Mo–Re alloy may vary. A chemical shift for molybdenum oxide is close to the published data for stable MoO_3. The intensity of the molybdenum oxide peaks and therefore oxygen concentration are significantly changed with film depth. Analysis of O 1s (not shown) and Re 4f peaks demonstrate that most of the oxygen is bound to molybdenum. The binding energy for the Re $4f_{7/2}$ peak is determined as 41.4 eV. The chemical shift of this peak is 1.3 eV, compared to pure Re and related to the Mo–Re compound.

Figure 5 shows wide scan XPS spectra of the 5.6 nm thick Mo–Re film. A signal from a sapphire substrate can be seen in figure 5(c). Spectra in figures 5(a)–(c) were obtained for etching times of 0, 90 and 360 min. High energy resolution

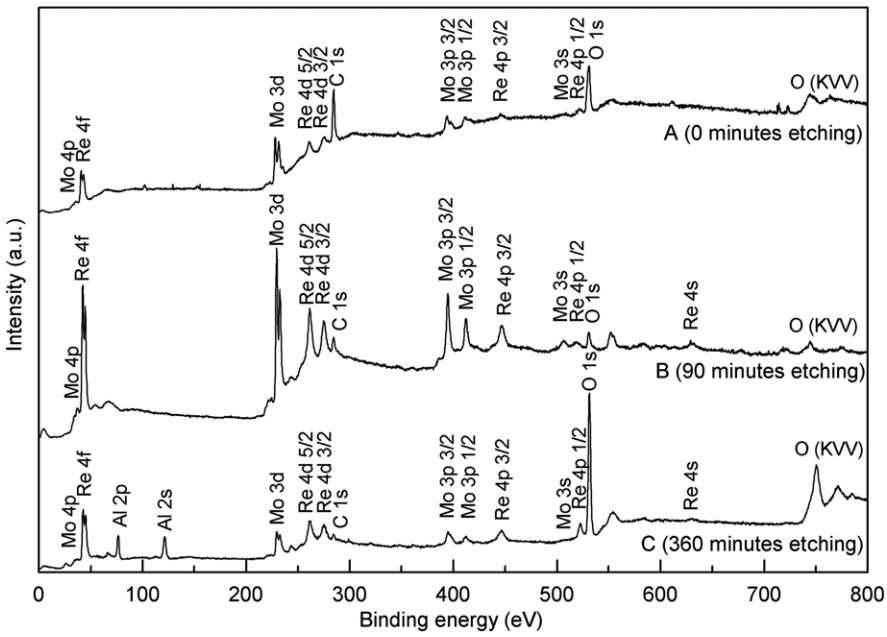

Figure 5. Wide scan XPS spectra of the 5.6 nm thick Mo–Re film after different sputtering times.

spectra of the same sample are given in figure 4 (graphs 3, 4 and 5, correspondingly).

The quantitative analysis of relative concentrations of components was performed using peak area sensitivity factors. Mo $3d_{5/2}$, Re $4f_{7/2}$, O 1s, C 1s, N 1s and Al 2p peaks were used for analysis of component concentrations.

The XPS analysis has shown that the Mo/Re atomic ratio in the films is 0.575/0.425; the films contain 10% of oxygen and less than 1% of other elements.

The XPS sputter depth profiling revealed diffusion of Mo atoms toward the film surface, which can be associated with the chemisorption of Mo by oxygen atoms adsorbed on the surface of the films with the following formation of a stable MoO_3 oxide. The study also revealed the diffusion of oxygen atoms from the sapphire substrate into the film with the subsequent formation of molybdenum oxides. Thus, the film interior is enriched in Re.

The XPS study also confirmed that deposited Mo–Re films were continuous.

The composition of the Mo–Re alloy target used for deposition of the films was also studied by XPS. The results show that the Mo/Re atomic ratio in the target was 0.588/0.412. Therefore the XPS data confirmed that the material transfer from the target to the substrate was nearly congruent. The oxygen is also present in the target in a concentration of about 3.5%. The content of other elements in the target was below 1%.

We also measured the film's sheet resistance R_s (by the standard four-probe method), superconducting transition temperature T_c, superconducting transition width ΔT_c and critical current density j_c at 4.2 K. Room temperature resistivity ρ of the films was defined as $\rho = R_s d$. The ratio of the room temperature resistivity to the resistivity at 20 K ($\rho_{300\ K}/\rho_{20\ K}$) for the investigated films was also measured. For DC characterization of the films, the microbridges 2 μm wide and 14 μm long were patterned by photolithography from 4 nm thick films. Electron diffusivity D was determined from the experimental data of the dependence of the second critical magnetic field on the temperature for these bridges. The experimental data of the parameters of Mo–Re films of different thicknesses are presented in table 3.

The best film quality of the film was achieved for 4 nm thick films ($T_c = 7.7$ K, $j_c(4.2\ K) = 1.1 \times 10^6$ A cm^{-2}, $D = 1.73$ cm^2 s^{-1}). These films meet the requirements for further development of superconducting single-photon detectors. Early experiments with 4 nm thick and 120 nm wide Mo–Re nanowires confirmed that a single-photon response can be obtained [20].

4. Conclusions

A technique for deposition of high-quality few-nm-thick Mo–Re films was developed. Films with thicknesses of 2–10 nm were deposited by the DC magnetron sputtering of the Mo(60)–Re(40) target in an argon atmosphere in the current stabilization mode. Mo–Re films demonstrated good superconducting properties, such as relatively high transition temperature and high critical current density. XPS investigation showed that the Mo/Re atomic ratio was 0.575/0.425 and the films contained 10% of oxygen and less than 1% of other elements. HRTEM analysis showed that the films had a homogeneous structure. The best quality of film was achieved for 4 nm thick Mo–Re films ($T_c = 7.7$ K, $j_c(4.2\ K) = 1.1 \times 10^6$ A cm^{-2}, $D = 1.73$ cm^2 s^{-1}). Ultrathin films can be used for Mo–Re SSPDs.

Acknowledgments

We would like to thank INTAS for the financial support within the project 'Superconducting Hot Electron Single-Photon Counter for Terahertz Radioastronomy' (grant

no. 03-51-4145). The ILTPE group acknowledges the support from the DFFD of Ukraine (grant no. F25/677-2007). MYM appreciates the personal support from the INTAS under YSF grant no. 04-83-3155. The authors would like to thank Dr A A Korneev for useful discussions.

References

[1] Gol'tsman G N, Smirnov K, Kouminov P, Voronov B, Kaurova N, Drakinsky V, Zhang J, Verevkin A and Sobolewski R 2003 *IEEE Trans. Appl. Supercond.* **13** 192
[2] Gol'tsman G N, Okunev O V, Chulkova G M, Lipatov A V, Semenov A D, Smirnov K V, Voronov B M and Dzardanov A L 2001 *Appl. Phys. Lett.* **79** 705
[3] Semenov A D, Gol'tsman G N and Korneev A A 2001 *Physica* C **351** 349
[4] Korneev A *et al* 2004 *Appl. Phys. Lett.* **84** 5338
[5] Korneev A *et al* 2005 *IEEE Trans. Appl. Supercond.* **15** 571
[6] Gol'tsman G *et al* 2007 *IEEE Trans. Appl. Supercond.* **17** 246
[7] Semenov A, Engel A, Hübers H-W, Il'in K and Siegel M 2005 *Eur. Phys. J.* **47** 495
[8] Zinoni C, Alloing B, Li L H, Marsili F, Fiore A, Lunghi L, Gerardino A, Vakhtomin Yu B, Smirnov K V and Gol'tsman G N 2007 *Appl. Phys. Lett.* **91** 1106
[9] Hadfield R, Habif J, Schlafer J, Schwall R and Nam S W 2006 *Appl. Phys. Lett.* **89** 1129
[10] Stevens M, Hadfield R, Schwall R, Nam S W, Mirin R and Gupta J 2006 *Appl. Phys. Lett.* **89** 1109
[11] Miki S, Fujiwara M, Sasaki M, Baek B, Miller A J, Hadfild R H, Nam S W and Wang Z 2008 *Appl. Phys. Lett.* **92** 1116
[12] Annunziata A J, Frydman A, Reese M O, Frunzio L, Rooks M and Prober D 2006 *Proc. SPIE* **6372** 63720V
[13] Verevkin A, Zhang J, Sobolewski R, Lipatov A, Okunev O, Chulkova G, Korneev A, Smirnov K, Gol'tsman G and Semenov A 2002 *Appl. Phys. Lett.* **80** 4687
[14] Gavaler J R, Janocko M A and Jones C K 1972 *Low Temperature Physics LT13* vol 3 (New York: Plenum) p 558
[15] Gavaler J, Santhanam A, Braginski A, Ashkin M and Janocko M 1981 *IEEE Trans. Magn.* **17** 573
[16] Talvacchio J, Janocko M A and Greggi J 1986 *J. Low Temp. Phys.* **64** 85
[17] Blaugher R D, Taylor A and Hulm J K 1962 *IBM J.* **6** 116–8
[18] Deambrosis S M, Keppel G, Ramazzo V, Roncolato C, Sharma R G and Palmieri V 2006 *Physica* C **441** 108
[19] Andreone A, Baldini A, Borchi E, Del Carmine P, Di Chiara A, Mando P A and Persico V 1995 *Nucl. Phys.* B **44** 688
[20] Milostnaya I *et al* 2008 *J. Low Temp. Phys* **151** 1573
[21] Voronov B M, Gershenzon E M, Goltsman G N, Serebryakova N A, Chinkova E V and Seidman L A 1994 *Superconductivity: Physics, Chemistry, Technique* **7** 1459
[22] Windt D L 1998 *Comput. Phys.* **12** 360